A Point Mutation of Tyr-759 in Interleukin 6 Family Cytokine Receptor Subunit gp130 Causes Autoimmune Arthritis

Toru Atsumi,[1,5] Katsuhiko Ishihara,[1,4] Daisuke Kamimura,[1] Hideto Ikushima,[1] Takuya Ohtani,[1] Seiichi Hirota,[2] Hideyuki Kobayashi,[6] Sung-Joo Park,[1] Yukihiko Saeki,[3] Yukihiko Kitamura,[2] and Toshio Hirano[1,4,5]

[1]*Department of Molecular Oncology (C7), the* [2]*Department of Pathology (C2), and the* [3]*Department of Molecular Medicine (C4), Graduate School of Medicine and the* [4]*Laboratory of Developmental Immunology, Graduate School of Frontier Biosciences, Osaka University, Suita, Osaka 565-0871, Japan*

[5]*Laboratory for Cytokine Signaling, RIKEN Research Center for Allergy and Immunology (RCAI), Yokohama, Kanagawa 230-0045, Japan*

[6]*Tokyo Research Laboratories, Kowa Co., Ltd, Higashi-murayama, Tokyo 189-0022, Japan*

Abstract

We generated a mouse line in which the src homology 2 domain–bearing protein tyrosine phosphatase (SHP)-2 binding site of gp130, tyrosine 759, was mutated to phenylalanine (*gp130*$^{F759/F759}$). The *gp130*$^{F759/F759}$ mice developed rheumatoid arthritis (RA)-like joint disease. The disease was accompanied by autoantibody production and accumulated memory/activated T cells and myeloid cells. Before the disease onset, the T cells were hyperresponsive and thymic selection and peripheral clonal deletion were impaired. The inhibitory effect of IL-6 on Fas ligand expression during activation-induced cell death (AICD) was augmented in *gp130*$^{F759/F759}$ T cells in a manner dependent on the tyrosine residues of gp130 required for signal transducer and activator of transcription 3 activation. Finally, we showed that disease development was dependent on lymphocytes. These results provide evidence that a point mutation of a cytokine receptor has the potential to induce autoimmune disease.

Key words: IL-6 • rheumatoid arthritis • gp130 • SHP-2 • STAT-3

Introduction

Rheumatoid arthritis (RA)* is a frequent autoimmune disorder; however, its etiology and pathogenesis are still not completely understood (1, 2). Genetic background and environmental factors, such as bacterial or viral infection, are thought to be involved in its onset. The genetic linkage of RA to an MHC class II molecule (HLA-DR) and the infiltration of T cells into the synovium of RA joints suggest that T cells are involved in the abnormal immune responses associated with RA (1). Proinflammatory cytokines, such as TNF-α, IL-1, and IL-6 are thought to play crucial roles in the pathology of RA and autoimmune diseases (3–5). Several engineered mutant mice that spontaneously develop arthritis have been reported. Analyses of the K/BxN TCR transgenic mouse showed that an autoantibody specific to a ubiquitous molecule can induce an organ-specific autoimmune disease (2, 6, 7). The HTLV-1 transgenic mouse is an animal model of arthritis that is triggered by viral infection (8). TNF-α transgenic mice and TNF AU-rich elements-deficient mice revealed that TNF-α is a pivotal cytokine for the induction of other proinflammatory cytokines and for the abnormal growth of synovial cells (9, 10). IL-1α transgenic mice (11) and gene targeting of an IL-1 receptor antagonist (12) indicated that the increased

T. Atsumi and K. Ishihara contributed equally to this work.

T. Ohtani's present address is the Dept. of Immunology, Institute of Geriatrics and Medical Science, Osaka City University School of Medicine, Osaka 545-8585, Japan.

Address correspondence to T. Hirano, Dept. of Molecular Oncology, C-7, Graduate School of Medicine, Osaka University, Suita, Osaka 565-0871, Japan. Phone: 81-6-6879-3880; Fax: 81-6-6879-3889; E-mail: hirano@molonc.med.osaka-u.ac.jp

**Abbreviations used in this paper:* AICD, activation-induced cell death; RA, rheumatoid arthritis; RAG, recombination activation gene; RF, rheumatoid factor; SEB, staphylococcal enterotoxin B; SHP, src homology 2 domain–bearing protein tyrosine phosphatase; SOCS, suppressor of cytokine signaling; STAT, signal transducer and activator of transcription; TRAP, tartrate-resistant acid phosphatase.

activity of a proinflammatory cytokine (IL-1) results in arthritis. The generation of RA-like joint diseases in a variety of engineered mutant mice may reflect the heterogeneity of human RA or the complicated mechanisms underlying the disease.

IL-6, which was originally identified as a B cell differentiation factor (13, 14), is now known to be a multifunctional cytokine that regulates the immune response, hematopoiesis, the acute phase response, and inflammation (4, 15). The first suggestion that IL-6 is involved in autoimmunity came from the finding that it is produced by cardiac myxoma cells, and patients with cardiac myxoma frequently show autoimmune symptoms (16). Since then, several pieces of evidence have been reported that suggest the involvement of IL-6 in autoimmune diseases, including RA (4, 17). Furthermore, IL-6 is required for experimentally induced autoimmune diseases or autoimmunity, including type II collagen- and antigen-induced arthritis (18–20), myelin oligodendrocyte protein-induced experimental autoimmune encephalomyelitis (21, 22), and pristane-induced autoantibody production (23). These results suggest that IL-6–dependent signaling pathways are involved in the pathogenesis of these experimentally induced autoimmune diseases. However, it is unknown whether IL-6 and its receptor system are involved in the pathogenesis of spontaneously occurring autoimmune diseases. The IL-6 receptor consists of an α chain and the subunit gp130. gp130 is shared by the receptors for IL-6 family cytokines, including leukemia inhibitory factor, ciliary neurotropic factor, oncostatin M, IL-11, and cardiotropin-1 (24). Binding of one of these cytokines to its receptor and gp130 activates JAK-1, JAK-2, and TYK-2, which phosphorylate tyrosine residues in the cytoplasmic domain of gp130. The transcription factor signal transducer and activator of transcription (STAT)-3 is recruited to the phosphorylated tyrosine residues in the YXXQ motif of gp130, where it is activated and dimerized, and subsequently enters the nucleus and regulates gene expression (24, 25). The src homology 2 domain–bearing protein tyrosine phosphatase (SHP)-2, is recruited to the phosphorylated tyrosine residue Y759 in gp130, where it becomes activated and forms a complex with the adaptor docking proteins, Gab1 and Gab2, leading to activation of the Ras–MAP kinase pathway (26). Several experiments in vitro have indicated that the SHP-2– and STAT-3–mediated signal-transduction pathways that are initiated through gp130 are involved in growth, differentiation, and gene expression in various cell lines (24, 25, 27, 28). SHP-2–mediated ERK mitogen-activated protein (MAP) kinase activation has been suggested to play negative roles in STAT-3–mediated biological responses (29, 30). Tyrosine residue Y759 also provides the binding site for the suppressor of cytokine signaling (SOCS)-3 protein, which negatively regulates the gp130 signals (31, 32). Recently, we generated a series of knock-in mouse lines in which the gp130-mediated SHP-2 or STAT-3 signals are selectively disrupted. To make the SHP-2 signal-deficient mice ($gp130^{F759/F759}$), we mutated Y759 of gp130 to phenylalanine (F759). The $gp130^{F759/F759}$ mice are born normal but develop splenomegaly, lymphadenopathy, and an enhanced acute phase reaction. In contrast, the STAT-3 signal-deficient mice ($gp130^{FXXQ/FXXQ}$) die perinatally, as do gp130-deficient mice ($gp130^{D/D}$). The embryonic fibroblasts from the $gp130^{F759/F759}$ mice show a severe reduction in ERK MAP kinase activation and prolonged STAT-3 activation after gp130 stimulation. The $gp130^{F759/F759}$ mice show increased production of Th1-type cytokines and Igs of the IgG2a and IgG2b classes, while these molecules are decreased in the $gp130^{FXXQ/FXXQ}$ immune system. These results indicate that the SHP-2–mediated or Y759-dependent signals negatively regulate the biological responses elicited by the STAT-3–mediated signals in vivo, and that the balance of positive and negative signals generated through gp130 is skewed or shifted to positive STAT-3 signaling in $gp130^{F759/F759}$ mice (33). Here we report that $gp130^{F759/F759}$ mice spontaneously developed arthritis in a manner dependent on lymphocytes accompanied by autoantibody production and T cell abnormalities at ~1 y of age. The $gp130^{F759/F759}$ mouse is thus a unique animal model in which a point mutation in a cytokine receptor results in a RA-like autoimmune disease.

Materials and Methods

Animals. The establishment of the $gp130^{F759/F759}$ knock-in mouse line was described previously (33). Heterozygous mice of a 129/C57BL/6 mixed background were intercrossed to obtain homozygous knock-in mice in the F3 generation, which were used for the studies described in this paper except for generating $gp130^{F759/F759}$ recombination activation gene (*RAG*)-$2^{-/-}$ mouse. $gp130^{F759/F759}$*RAG-2*$^{-/-}$ mouse was generated by crossing $gp130^{F759/F759}$ mouse with *RAG-2*–deficient mouse of 129S6/C57BL/6F1 background. To make a F1 generation of *RAG-2*–deficient mouse in a C57BL/6 and 129S6/SvEv background, we obtained *RAG-2*–deficient mouse, that had been backcrossed to C57BL/6 eight times, and *RAG-2*–deficient mouse with a 129S6/SvEv background from M. Itoh (Laboratory of Immunology, Central Institute for Experimental Animals, Kanagawa, Japan) and Taconic, respectively. To obtain lymphocytes from $gp130^{FXXQ/FXXQ}$ mice, which die as neonates, we reconstituted lethally irradiated mice with liver cells from $gp130^{FXXQ/FXXQ}$ fetuses that were harvested at 14.5 d after coitus, as described previously (reconstituted mice; reference 33). These mice were kept at the Institute of Experimental Animal Sciences at Osaka University Medical School.

Detection of Igs and Autoantibodies in Sera. To analyze the relationship between the serum antibody levels including autoantibodies, severity of the arthritis, and sex differences, we collected sera from $gp130^{F759/F759}$ mice with arthritis and $gp130^{WT/WT}$ mice of both sexes at 11–12 mo old (male $gp130^{F759/F759}$, $n = 14$; female $gp130^{F759/F759}$, $n = 17$; male $gp130^{WT/WT}$, $n = 8$; and female $gp130^{WT/WT}$, $n = 8$). Serum levels of total Igs were determined by an isotype-specific ELISA as described previously (34). Rheumatoid factor (RF) for mouse Ig of both IgM and IgG classes, anti-dsDNA, and anti–ssDNA antibodies were measured using commercial ELISA kits (Shibayagi, Japan). An ELISA kit for anti-nRNP antibody was purchased from Alpha Diagnostic. To detect RF, 100 μl of 200-fold diluted serum was added to each well of the ELISA plate precoated with Fc fragments of mouse IgG. The plates were incubated for 2 h and washed three times

with washing buffer. Then, horseradish peroxidase–labeled goat anti–mouse IgG, which was deprived of anti–mouse Fc antibodies by extensive absorption, was added. After 2 h incubation, the plates were washed three times, substrate was added and the absorbance at 450 nm was measured by the microplate reader.

Clinical Assessment of Arthritis. The mice were assessed by two independent observers for signs of arthritis: redness, swelling, and restriction of mobility. The severity of the arthritis was based on five signs, which were each assessed bilaterally: (1) swelling of digits of the forelimb; (2) swelling of the footpad; (3) swelling of the ankle; (4) restriction of mobility of the wrist joint; and (5) restriction of mobility of the ankle joint. The severity of the arthritis was graded on a scale of 0–2 for each of the five conditions as follows: 0 (no change); 1 (mild change); and 2 (severe change). The severity score shown in Fig. 1 b is a sum of the scores for the five signs, assessed bilaterally, to give a possible maximum of 20 points for each mouse. The incidence was expressed as the percentage of mice that showed visible arthritis.

Radiology and Histology. X-ray photographs of the bones were taken using a SOFTEX CMB-2 (SOFTEX Co., Ltd.) and Fuji Film. For the histologic examination, joints were fixed in 4% paraformaldehyde, decalcified in 10% EDTA-4Na, and embedded in paraffin. Sections were stained with H&E. For the tartrate-resistant acid phosphatase (TRAP) staining, naphthol AS-BI phosphate (Sigma-Aldrich) was used according to the manufacturer's instructions, and the sections were counterstained with hematoxylin.

Quantitative Analysis of Gene Expression. Total RNA was isolated from the joints or activated T cells using sepasol–RNA I (Nakarai Tesque), or RNeasy mini kit (QIAGEN). For RT-PCR analysis, 3–5 μg of total RNA was digested with RNase-free DNaseI. First-strand cDNAs were synthesized using $Oligo(dT)_{12–18}$ Primer and SuperScriptII $RNaseH^-$ reverse transcriptase (GIBCO BRL). To detect corresponding cytokine mRNAs by RT-PCR, specific primers and probes reported previously were used (35). The specific primer pairs for FasL and SOCS-3 were as follows: FasL 5′-CTGGGTTGTACTTCGTGTATTCCA-3′ and 5′-TCCTCCATTAGCACCAGATCCT-3′ and SOCS-3: 5′-GCGAGAAGATTCCGCTGGTA-3′ and 5′-CGTTGACAGTCTTCCGACAAA-3′. PCR reactions were performed in the GeneAmp 5700 Sequence Detection System (Applied Biosystems). The relative amounts of transcripts were normalized to the HPRT transcript.

FACS® Analysis. Flow cytometry analysis was performed as described previously (36), and analyzed using a FACSCalibur™ flow cytometer (Becton Dickinson). mAbs used are as follows: FITC-anti-IgM (AM/3); FITC-anti-CD44 (IM7); FITC-anti-CD25 (PC61); FITC-anti-Gr-1 (RB6–8C5); FITC-anti-TCR-α for HY (T3.70, a gift from Y. Takahama, RIKEN Research Center for Allergy and Immunology, Tokushima, Japan); PE-anti-IgD (11–26c); PE-anti-CD62L (MEL14); PE-anti-CD69 (H1.2F3); PE-anti-Syndecan-1 (281–2); Quantum Red-anti-CD8α (53–6.7); or APC-anti-CD4 (CT-CD4), APC-anti-CD11b (M1/70), and APC-anti-CD45R (RA3–6B2). To avoid the contamination of peripheral T cells, the thymus from old mice was carefully taken out after removal of the parathymic lymph nodes. Furthermore, we examined a part of the sample histologically.

Cell Proliferation Assay. Thymocytes or lymph node cells were cultured at 5×10^5 cells per well or 2×10^5 cells per well, respectively, in 96-well plates for 48 or 72 h, in RPMI 1640 containing 10% FCS and 50 μM 2-mercaptoethanol, in the presence of various concentrations of a hamster anti–mouse CD3ε antibody (clone 145–2C11). ^{3}[H]thymidine (0.5 μCi per well) was pulsed for the last 6 h of incubation, and incorporation was measured with a micro β-counter.

Analysis of Thymic Selection Using Anti-HY TCR Transgenic Mice. Anti-HY TCR transgenic mice were purchased from Taconic and mated with *gp130$^{F759/F759}$* mice to obtain the F1 generation. Anti-HY TCR gene expression was detected by staining peripheral blood cells with the anticlonotypic antibody, FITC-T3.70. F1 mice were intercrossed to obtain anti-HY TCR^+ *gp130$^{WT/WT}$* and anti-HY TCR^+ *gp130$^{F759/F759}$* mice of both sexes. Thymocytes of 6–8-wk-old mice were stained with FITC-T3.70, PE-anti-CD4 (RM4–5), Quantum Red-anti-CD8α, and $T3.70^+$ thymocytes were analyzed with a FACSCalibur™ flow cytometer.

Clonal Deletion In Vivo by Staphylococcal Enterotoxin B. Staphylococcal enterotoxin B (SEB) (100 μg) (Toxin Technology) was injected intraperitoneally into 6-wk-old mice on day 0. T cell subsets in the peripheral blood were analyzed by flow cytometry on days 0, 3, 7, and 14. Cells were stained with FITC-anti-Vβ8.1/8.2 (clone MR5–2) or FITC-anti-Vβ6 (clone RR4–7), Quantum Red-anti-CD8α and APC-anti-CD4.

Induction and Analysis of Apoptosis. Lymph nodes T cells were negatively enriched (purity ≥ 96%) using magnetic beads conjugated with anti-MHC class II antibody and a Midi MACS® column (Miltenyi Biotec). Purified T cells (5×10^5 cells per milliliter) were stimulated with plate-immobilized 5 μg/ml anti-CD3 antibody, 2 μg/ml anti-CD28 antibody (clone 37.51; BD PharMingen), and 50 U/ml rIL-2 for 48 h. The cells were harvested, washed, and replated at 3×10^5 cells per milliliter for a further 48 h in the presence of rIL-2 to prepare the activated T cells for activation-induced cell death (AICD) induction. They were then harvested, and the dead cells were removed using Histopaque 1083 (Sigma-Aldrich) following the manufacturer's instructions. To induce AICD, the viable activated T cells were cultured at 10^6 cells per milliliter with plate-immobilized anti-CD3 in the presence or absence of 20 ng/ml IL-6. 2 h later, some T cells were harvested and the total RNA was isolated using an RNeasy Mini kit (QIAGEN) for quantitative RT-PCR as described above. 8 and 20 h later, a part of T cell culture was used for staining with the following antibodies: FITC-anti-CD4 (RM4–4); PE-anti-FasL (MFL3; BD PharMingen); 7-AAD; and Cy5-AnnexinV, and analyzed with a FACSCalibur™ flow cytometer.

Western Blot Analysis. Activated T cells for AICD were stimulated with 20 ng/ml IL-6 at 37°C for 30, 60, 120, and 180 min. Cell lysis and Western blot analysis were performed as described previously (33). Anti–phospho-JAK-1 (Biosource), anti-phospho-STAT-3 (New England Biolabs), and anti–STAT-3 antibodies (New England Biolabs) were used in this study.

Statistical Analysis. Statistical analyses for growth responses, numbers of $T3.70^+CD8^+$ thymocytes, and SEB-induced clonal deletion were performed by Student's *t* test. Serum levels of Igs and autoantibodies in male and female *gp130$^{F759/F759}$* mice and quantitative analysis of cytokine mRNA expression were analyzed by Mann-Whitney U test. Correlation between serum autoantibody levels and severity scores was examined using Spearman's rank correlation. $P < 0.05$ is thought as significant.

Results

Spontaneous Development of Arthritis in gp130$^{F759/F759}$ Mice. By as early as 8 mo, the *gp130$^{F759/F759}$* mice showed swelling and redness of the paws and limited mobility of the ankle or wrist joints (Fig. 1 d). Neither wild-type nor

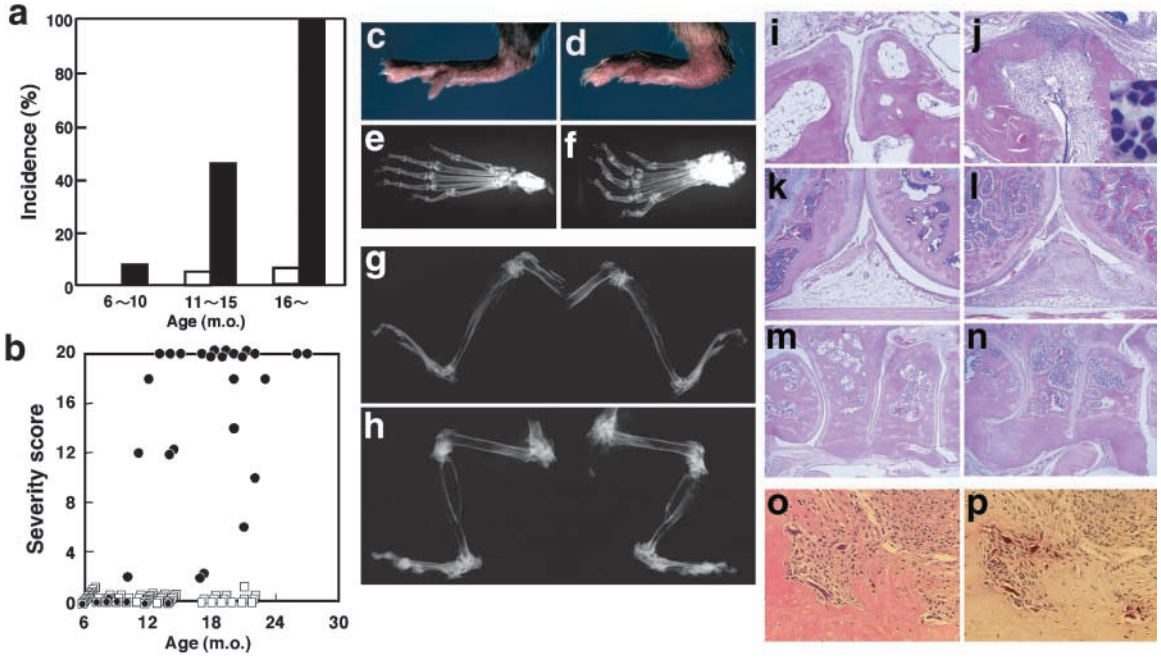

Figure 1. Development of spontaneous arthritis in gp130$^{F759/F759}$ mice. (a) Incidence of arthritis in *gp130*$^{F759/F759}$ mice of three age groups. Each joint of *gp130*$^{WT/WT}$ (male $n = 26$, female $n = 23$) and *gp130*$^{F759/F759}$ (male $n = 29$, female $n = 15$) mice was regularly examined and the severity was scored according to a set of defined criteria (see Materials and Methods). White and black bars indicate the incidence of arthritis in *gp130*$^{WT/WT}$ and *gp130*$^{F759/F759}$ mice of each age group, respectively. (b) Relationship between age and severity of arthritis in *gp130*$^{F759/F759}$ (black circle: male $n = 29$, female $n = 15$) and control *gp130*$^{WT/WT}$ (white square, male $n = 26$, female $n = 23$) mice. (c) Hindlimb of an 11-mo-old *gp130*$^{WT/WT}$ mouse. (d) Swelling and redness of the hindlimb of an 11-mo-old *gp130*$^{F759/F759}$ mouse. (e and f) Radiologic analysis of hindlimbs from *gp130*$^{WT/WT}$ (e) and *gp130*$^{F759/F759}$ (f) mice. Representative cases (18 mo old) from the radiological analysis of 18 mice with arthritis are shown. (g and h) Control *gp130*$^{WT/F759}$ mouse (g) and ankylosis of the large joints of a *gp130*$^{F759/F759}$ mouse (h) (28 mo old). (i–p) Histological analyses of H&E-stained sections of joints. Ankle joints of *gp130*$^{WT/WT}$ (i) and *gp130*$^{F759/F759}$ (j) mice. Inset in (j) shows infiltration of neutrophils in the synovium in larger magnification. Knee joints of *gp130*$^{WT/WT}$ (k) and *gp130*$^{F759/F759}$ (l) mice. Ankylotic ankle joint of *gp130*$^{F759/F759}$ (n) mouse, whose X-ray photographs are shown in (h), and a control *gp130*$^{WT/F759}$ (m) mouse. (o) Pannus formation and activated osteoclasts in the ankle joint of a *gp130*$^{F759/F759}$ mouse. (p) TRAP staining of a serial section from the section used in (o) with hematoxylin counter staining. Representative cases from the histological analysis of *gp130*$^{F759/F759}$ mice with arthritis ($n = 18$) are shown.

gp130$^{WT/F759}$ littermates showed these symptoms (Fig. 1 c). The incidence of arthritis was ∼45% in the *gp130*$^{F759/F759}$ mice at 11–15 mo of age and reached 100% in those older than 16 mo (Fig. 1 a). The severity scores, which were assessed by the criteria defined in Materials and Methods, were higher in older mice (Fig. 1 b). In addition, the larger joints, such as the elbows and knees, were affected symmetrically in many diseased mice and became rigid. Thus, the arthritis observed in *gp130*$^{F759/F759}$ mice was chronic and progressive. The *gp130*$^{F759/F759}$ mice backcrossed to C57BL/6 eight times developed essentially similar arthritis as *gp130*$^{F759/F759}$ mice of a 129/C57BL/6 mixed background that we used in this study (unpublished data).

There was no significant difference in the final incidence between males and females; however, in females the onset of arthritis tended to be earlier (unpublished data). Actually, when the severity scores of mice with arthritis at ages 11–12 mo old were analyzed, the score was significantly higher in females than males; (average score ± SEM: female, 13.5 ± 1.3, $n = 17$; male, 9.6 ± 0.9, $n = 14$; $P < 0.05$), suggesting that the hormonal environment somehow affects the severity of arthritis in *gp130*$^{F759/F759}$ mice. In histologic examination, the *gp130*$^{F759/F759}$ mice showed severe synovitis with destructive changes at multiple joints.

Representative histology results are shown in Fig. 1, i–p. In the ankle joint of *gp130*$^{F759/F759}$ mice, marked proliferation of the synovium with pannus formation accompanied by the infiltration of inflammatory cells, predominantly neutrophils (Fig. 1 j, inset), with fibrin deposits and severe bone destruction were observed (Fig. 1 j, and control, i). At the site of bone erosion, activated osteoclasts, which were identified as TRAP$^+$ multinucleated cells, were observed (Fig. 1, o and p). The knees were also affected (Fig. 1 l and control, k). In the mice with rigid ankles and toes, a severe narrowing of joint spaces and ankylosis were observed (Fig. 1 n and control, m).

In radiologic examinations, generalized osteoporosis and marked joint destruction were noted in all limbs. The phalangeal and tarsal bones were destroyed, and prominent bone fusions and reactive sclerotic changes in the tarsal bones were observed (Fig. 1 f, and control, e). In addition, severe joint destruction and ankylosis were also observed in the larger bilateral joints such as the ankles, knees, and hips (Fig. 1 h, and control, g). All these clinical, histologic, and radiologic findings in the *gp130*$^{F759/F759}$ mice resemble those of human RA, although some differences were observed, such as the relatively small number of infiltrated lymphocytes and plasma cells in the mice. Quantitative

RT-PCR analysis of cytokine transcripts in the joints of the *gp130$^{F759/F759}$* mice revealed significantly higher transcriptional levels of IL-6 (fold ± SEM; 24 ± 9, $P < 0.05$) than in controls. Although it was not statistically significant, some cases of arthritis mice showed elevated transcriptional levels of IL-1β (2.4 ± 0.7), IL-10 (3.6 ± 1.0), and TNF-α (1.8 ± 0.9). Thus, the balance of the local cytokine production tended to become skewed toward a proinflammatory status.

Autoantibody Production in gp130$^{F759/F759}$ Mice. Spontaneous development of RA-like arthritis in *gp130$^{F759/F759}$* mice prompted us to examine autoantibody production of mice with arthritis. At the age of 9 wk, the serum Ig levels of all isotypes in the *gp130$^{F759/F759}$* Igs were similar to those in wild-type littermates (33). However, at 11–12 mo of age, serum Igs were slightly increased in *gp130$^{F759/F759}$* mice with arthritis. The serum levels of IgG1 (average OD ± SEM: male, *gp130$^{F759/F759}$*, 0.37 ± 0.01; *gp130$^{WT/WT}$*, 0.31 ± 0.02, $P < 0.05$, female, *gp130$^{F759/F759}$*, 0.40 ± 0.01; *gp130$^{WT/WT}$*, 0.23 ± 0.02, $P < 0.01$) and IgA (male, *gp130$^{F759/F759}$*, 0.32 ± 0.01; *gp130$^{WT/WT}$*, 0.26 ± 0.01, $P < 0.01$, female, *gp130$^{F759/F759}$*, 0.33 ± 0.01; *gp130$^{WT/WT}$*, 0.26 ± 0.02, $P < 0.01$) were increased in both male and female *gp130$^{F759/F759}$*. IgG2a in female (*gp130$^{F759/F759}$*, 0.24 ± 0.01; *gp130$^{WT/WT}$*, 0.19 ± 0.01, $P < 0.01$) and IgG2b in male (*gp130$^{F759/F759}$*, 0.38 ± 0.00; *gp130$^{WT/WT}$*, 0.32 ± 0.02, $P < 0.05$) were a little bit increased.

There was no significant difference in the increase of serum Ig levels between male and female *gp130$^{F759/F759}$* mice (unpublished data) except for IgG1 (male, 0.37 ± 0.01; female, 0.40 ± 0.01, $P < 0.05$). More importantly, the 11–12-mo-old *gp130$^{F759/F759}$* mice produced significantly higher levels of autoantibodies, such as RF of the IgG class, anti–single-strand DNA (anti-ssDNA), anti–double-strand DNA (anti-dsDNA), and anti-ribonuclear protein (anti-nRNP) antibodies, all of which were significantly higher in females than males: IgG-RF (average of OD ± SEM for males 0.10 ± 0.03, and females 0.20 ± 0.05, $P < 0.01$), anti-ssDNA antibody (0.33 ± 0.14, and 1.40 ± 0.27, $P < 0.01$), anti-dsDNA antibody (0.20 ± 0.08 and 0.83 ± 0.18, $P < 0.01$) and anti-nRNP antibody (0.88 ± 0.11, and 1.49 ± 0.16, $P < 0.01$) (Fig. 2). These results suggest that the abnormal gp130 signals broke the homeostasis of the immune system and elicited autoimmunity. However, there were neither proteinuria nor pathological changes in the kidney (unpublished data).

Then, we statistically examined the correlation between the severity and the level of each autoantibody in females and males. However, there was no correlation between the level of each autoantibody and severity score. Some *gp130$^{F759/F759}$* mice had sporadic elevation of the serum IgM-RF, being not correlated with severity score (unpublished data). We also examined the correlation between the level of each autoantibody in males and females; IgG-RF versus IgM-RF, IgG-RF versus anti-ssDNA, IgG-RF versus anti-dsDNA, IgG-RF versus anti-nRNP, anti-ssDNA versus anti-dsDNA, and anti-dsDNA versus anti-nRNP. Among them, there were correlations in IgG-RF versus anti-ssDNA ($r = 0.54$, $P < 0.05$), IgG-RF versus anti-nRNP ($r = 0.67$, $P < 0.01$), and anti-ssDNA versus anti-dsDNA ($r = 0.84$, $P < 0.01$) in females. In males, only anti-ssDNA versus anti-dsDNA showed correlation ($r = 0.99$, $P < 0.01$). These results suggest that the hormonal environment affects the autoimmunity in *gp130$^{F759/F759}$* mice.

Increase in Activated T Cells and Myeloid Cells in the Lymphoid Organs of gp130$^{F759/F759}$ Mice. To understand the involvement of the immune system in the arthritis of the *gp130$^{F759/F759}$* mice, we first analyzed the cell populations in their lymphoid organs compared with those of their *gp130$^{F759/WT}$* littermates. Analysis of the thymus of the diseased mice revealed a lower frequency of CD4/CD8 double-positive cells and a higher frequency of CD4/CD8 double-negative cells and CD4 or CD8 single-positive cells than their *gp130$^{F759/WT}$* littermates (Fig. 3 a). The population of CD4/CD8 double-negative cells included IgM^{lo}

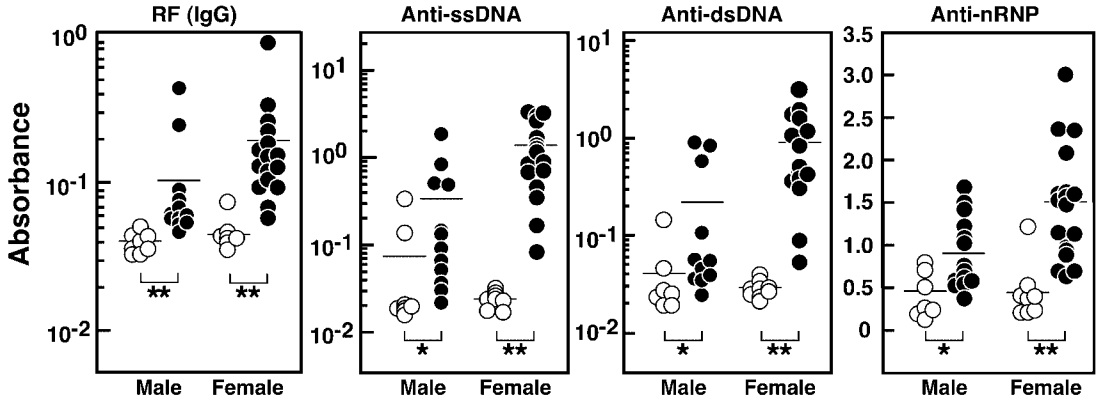

Figure 2. Autoantibody production in gp130$^{F759/F759}$ mice. Serum from 11–12-mo-old *gp130$^{F759/F759}$* mice with arthritis ($n = 31$; 14 male, 17 female) and their wild-type littermates ($n = 16$; 8 male, 8 female) was assayed for the levels of autoantibodies by ELISA. White and black circles represent the serum levels of antibody in individual *gp130$^{WT/WT}$* and *gp130$^{F759/F759}$*mouse, respectively. Horizontal bars represent the mean values of each group. Asterisks indicate significant differences by Mann-Whitney U test (*$P < 0.05$; **$P < 0.01$).

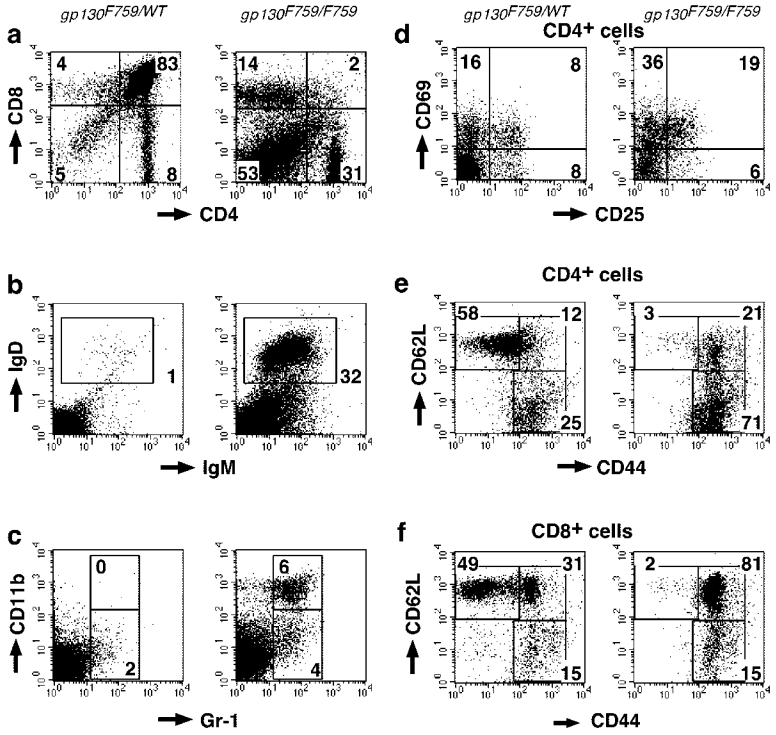

Figure 3. Flow cytometry analysis of lymphoid organs of gp130$^{F759/F759}$ mice with arthritis. Cells from the thymus and lymph nodes of a *gp130*$^{F759/F759}$ mouse with arthritis and a *gp130*$^{F759/WT}$ littermate at 19 mo of age were stained with a combination of antibodies and analyzed as described in Materials and Methods. Dot plots of thymocytes (a and b), total lymph node cells (c), CD4$^+$ (d and e), and CD8$^+$ (f) lymph node cells are shown. The numbers indicate the frequencies of the cell populations in the indicated regions of the dot plots. These are representative data of severe cases from the flow cytometry analysis of *gp130*$^{F759/F759}$ mice with arthritis (n = 27) and control mice (n = 15) at ages from 8 to 30 mo. The results from the *gp130*$^{WT/WT}$ mice were similar to those from the *gp130*$^{F759/WT}$ mice.

IgD^{hi} conventional B cells, CD45R$^+$Syndecan-1$^+$ plasma cells, and CD11b$^+$ (Gr-1$^+$ and Gr-1$^-$ cells (Fig. 3 b and unpublished data). These abnormalities of thymic populations expressing CD4 or CD8 were present to various degrees in 80% (16 out of 20) of the mice with arthritis. The lower frequency of CD4/CD8 double-positive cells and the higher frequency of CD4 or CD8 single-positive cells in the thymus were unlikely to be due to the stress experienced by the mice with arthritis, because these differences began to be observed in *gp130*$^{F759/F759}$ mice as young as 18 wk old, before the onset of the arthritis (unpublished data).

In the lymph nodes of the *gp130*$^{F759/F759}$ mice with arthritis, the numbers of myeloid cells, especially Gr-1$^+$ CD11b$^+$ cells (Fig. 3 c), were higher to various degrees. Correlating with the level of increase in the number of neutrophils, B cells were relatively fewer in the mice with arthritis (unpublished data). The number of B-1 cells was not higher in the spleens of the mice with arthritis. Although the ratio of CD4 to CD8 T cells showed no consistent changes, the CD62L$^+$CD44$^-$ naive T cell subset was almost completely absent in the populations of both CD4$^+$ and CD8$^+$ T cells (Fig. 3, e and f). Instead, the numbers of CD62L$^-$CD44$^+$ memory/activated T cells and CD62L$^+$ CD44$^+$ T cells were higher in the CD4$^+$ and CD8$^+$ T cell populations, respectively. The activated status of the T cells in the arthritic mice was further indicated by the higher numbers of CD4$^+$ T cells expressing CD69 or CD25, which are early activation markers (Fig. 3 d). The number of CD8$^+$ T cells expressing CD69 or CD25, however, was rarely higher in the arthritic mice (unpublished data). These differences were also observed in the spleen, indicating that the peripheral T cells, especially the CD4$^+$ T cells, were chronically activated in the *gp130*$^{F759/F759}$ mice with arthritis.

Hyperresponsiveness of Thymocytes and Lymph Node T Cells in Young gp130$^{F759/F759}$ *Mice.* The flow cytometry analysis indicated no abnormalities in the major population or surface markers of lymphoid cells from *gp130*$^{F759/F759}$ mice younger than 12-wk-old (Fig. 4, a and b, top). However, the anti-CD3 antibody-induced T cell growth responses were much higher in the thymocytes and lymph node cells of young *gp130*$^{F759/F759}$ mice than in wild-type mice (Fig. 4, a and b, bottom), indicating that the functional abnormality of the T cells was present in the *gp130*$^{F759/F759}$ mice even before disease onset.

Impairment of Thymic Negative Selection and Clonal Deletion in the Peripheral T Cells of gp130$^{F759/F759}$ *Mice In Vivo.* Both central and peripheral tolerances play crucial roles in maintaining self-tolerance (37, 38). We crossed *gp130*$^{F759/F759}$ mice with anti–HY-TCR transgenic mice to examine the effect of the *gp130*$^{F759/F759}$ mutation on thymic selection (39). In the female anti-HY-TCR$^+$ *gp130*$^{F759/F759}$ thymocytes, the frequency of CD8$^+$ cells was similar to anti-HY-TCR$^+$ *gp130*$^{WT/WT}$ thymocytes (Fig. 5 a, top), indicating that positive selection was not impaired. In the male anti–HY-TCR$^+$ *gp130*$^{F759/F759}$ thymocytes, a severe reduction in total cell number and CD4/CD8 double-positive cells was observed, similar to that seen in anti-HY-TCR$^+$ *gp130*$^{WT/WT}$ thymocytes, but the number of CD8^{lo} thymocytes (Fig. 5 a, left and right bottom; in the upper left quadrant and Fig. 5 b), which are thought to be the thymocytes that have escaped negative selection (40), was higher in *gp130*$^{F759/F759}$ mice, indicating that the negative selection in *gp130*$^{F759/F759}$ mice was impaired to some ex-

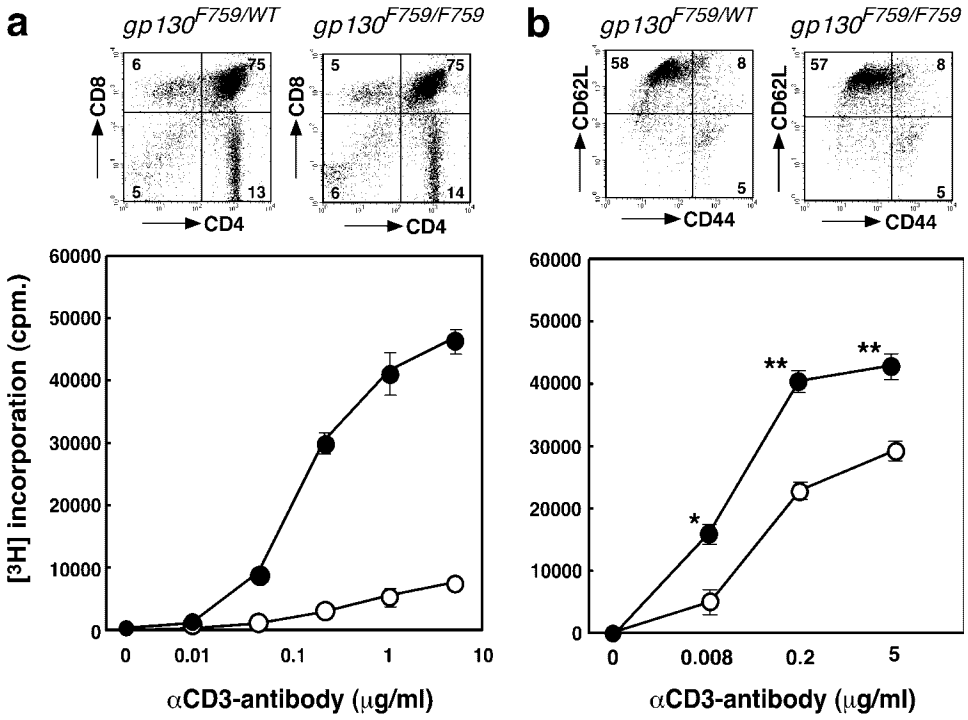

Figure 4. Hyperresponsiveness of anti-CD3–stimulated thymocytes and lymph nodes T cells in gp130$^{F759/F759}$ mice (a) Thymocytes from 12-wk-old *gp130$^{F759/F759}$* mice without arthritis (black circles) and their littermates (white circles) were cultured for 48 h in the presence of the indicated concentrations of soluble anti-CD3 antibody. Growth responses were measured by ^{3}[H]thymidine incorporation. Error bars indicate the SD of duplicated cultures. Representative data from three independent experiments are shown. The populations of the thymocytes used in this growth assay were analyzed by flow cytometry and dot plots are shown on the top. (b) Lymph node cells from 8-wk-old *gp130$^{F759/F759}$* mice without arthritis (black circles) and their littermates (white circles) were cultured for 72 h in the presence of the indicated concentrations of soluble anti-CD3 antibody. Error bars indicate the SD of duplicated cultures. Asterisks indicate significant differences by Student's *t* test ($P < 0.05$). Expression of markers for memory/activated T cells in the lymph node cells used in this experiment is shown on the top. Representative data from >10 independent experiments are shown.

tent. Then, we examined the effects of the Y759 mutation on the peripheral clonal deletion of activated T cells. For this study we injected a superantigen, SEB, into the mice (41). The frequency of Vβ8-positive peripheral blood T cells that had been specifically activated by SEB was decreased by deletion in wild-type mice injected with SEB. On the other hand, the frequency of Vβ8^{+}CD4^{+}T cells in the *gp130$^{F759/F759}$* mice was not reduced (Fig. 6 a). The frequency of Vβ6^{+}CD4^{+}T cells that had not been activated by SEB showed no reduction in either *gp130$^{F759/F759}$* or wild-type mice (Fig. 6 b). These results indicated that both thymic selection and clonal deletion of peripheral T cells were impaired in the *gp130$^{F759/F759}$* mice.

Inhibitory Effect of IL-6 on Fas Ligand Expression Was Augmented in gp130$^{F759/F759}$ T Cells During AICD. The accumulation of activated T cells in the lymphoid organs and resistance to SEB-induced peripheral clonal deletion in *gp130$^{F759/F759}$* mice suggested that AICD is impaired in *gp130$^{F759/F759}$* T cells. Anti-CD3 antibody induced similar levels of AICD (~50%) in both *gp130$^{F759/F759}$* and control T cells. In the presence of IL-6, anti-CD3–induced AICD was inhibited and this inhibitory effect was, however, higher in *gp130$^{F759/F759}$* T cells than wild-type T cells (Fig. 7 a). To identify molecules responsible for the IL-6-dependent resistance to AICD, we first examined the expression of molecules related to activation and apoptosis in the primed T cells. The expression levels of Fas, CD25, CD69, Bcl-2, and Bcl-X before and after the induction of AICD were similar in wild-type and *gp130$^{F759/F759}$* T cells (unpublished data). The expression of FasL on *gp130$^{F759/F759}$* T cells stimulated with the anti-CD3 antibody alone was similar to wild-type T cells. Addition of IL-6 to anti-CD3 stimulation only slightly decreased the frequency of FasL-positive cells (22–18%) in wild-type T cells (Fig. 7 b). This negative effect of IL-6 was more evident in *gp130$^{F759/F759}$* T cells (20–10%) than in wild-type T cells. A similar negative effect of IL-6 on FasL expression was observed at the transcription level (Fig. 7 c), but IL-6 had no effect on the anti-CD3–induced upregulation of IL-2 mRNA (unpublished data). To understand the molecular mechanisms of the negative effect of IL-6 on FasL expression, we examined whether the gp130-mediated signals in *gp130$^{F759/F759}$* T cells were abnormal in any way.

As shown in Fig. 7 d, the IL-6–induced tyrosine-phosphorylation of JAK-1 and STAT-3 was prolonged, compared with wild-type T cells, consistent with the previous results observed in *gp130$^{F759/F759}$* fibroblasts (33). Furthermore, RT-PCR analysis revealed that IL-6 induced SOCS-3 but not SOCS-1 mRNA in the activated *gp130$^{F759/F759}$* T cells, and that this induction of SOCS-3 in the activated *gp130$^{F759/F759}$* T cells was enhanced as compared with *gp130$^{WT/WT}$* T cells, probably reflecting the increased STAT-3 activation (Fig. 7 e, and unpublished data). These results raised the possibility that a prolonged activation of STAT-3 might interfere with FasL expression. To test this possibility, we used T cells purified from reconstituted mice (Materials and Methods) with *gp130$^{FXXQ/FXXQ}$* fetal liver cells, which express gp130 mutated at the four tyrosine residues required for gp130-mediated STAT-3 activation. As shown in Fig. 7 d, IL-6 did not induce tyro-

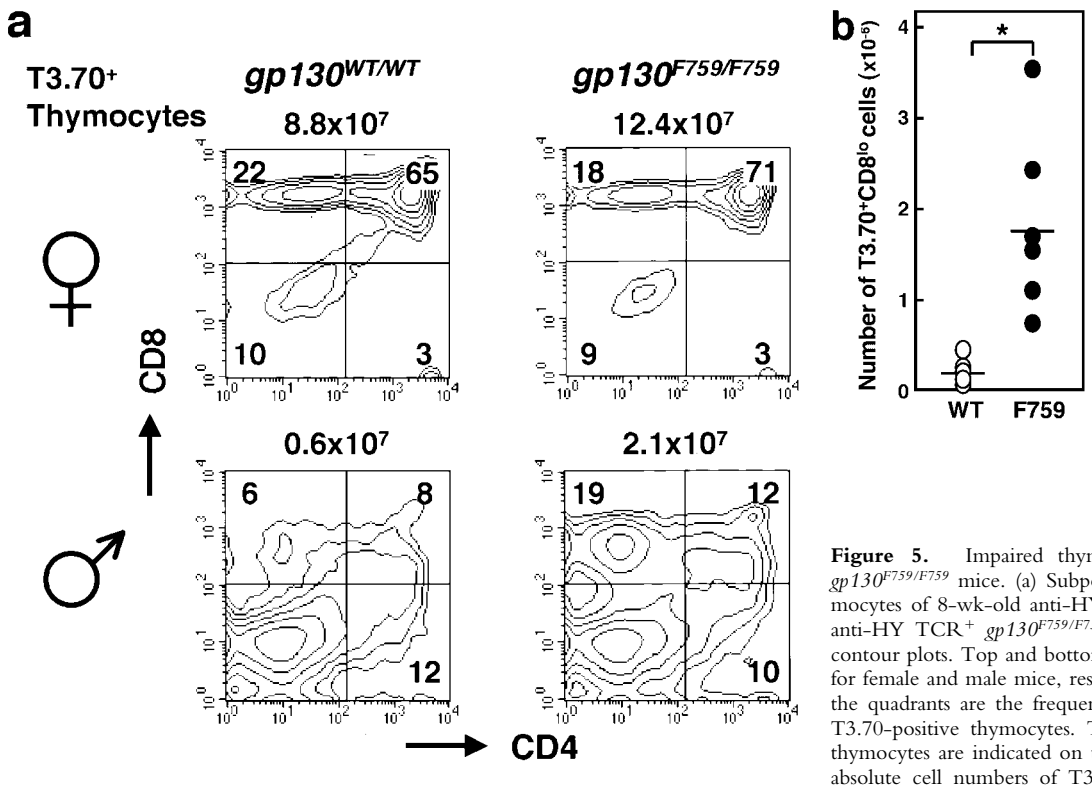

Figure 5. Impaired thymic negative selection in $gp130^{F759/F759}$ mice. (a) Subpopulations of T3.70$^+$ thymocytes of 8-wk-old anti-HY TCR$^+$ $gp130^{WT/WT}$ and anti-HY TCR$^+$ $gp130^{F759/F759}$ mice are shown in the contour plots. Top and bottom panels show the analysis for female and male mice, respectively. The numbers in the quadrants are the frequencies of the subsets in the T3.70-positive thymocytes. The total cell numbers of thymocytes are indicated on the contour plots. (b) The absolute cell numbers of T3.70$^+$CD8^{lo} thymocytes of male anti-HY TCR$^+$ $gp130^{WT/WT}$ (white circle), ($n = 6$) and anti-HY TCR$^+$ $gp130^{F759/F759}$ (black circle), ($n = 6$) mice are shown. Asterisk indicates significant differences by Student's t test (*$P < 0.05$). Representative data from three independent experiments are shown.

sine-phosphorylation of STAT-3 in these T cells. Furthermore, the negative effect of IL-6 on AICD and FasL expression was not observed in $gp130^{FXXQ/FXXQ}$ T cells (Fig. 7, a–c). Taken together, these results strongly suggest that gp130-mediated STAT-3 activation plays a negative role in the anti-CD3–induced upregulation of FasL in activated T cells.

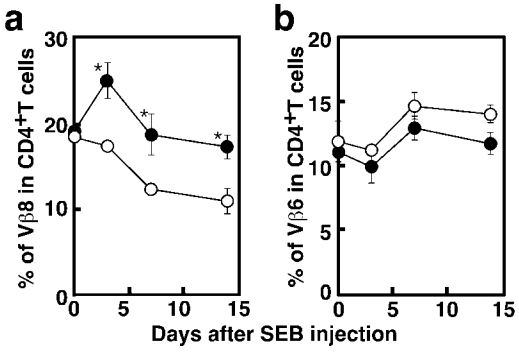

Figure 6. Impaired peripheral clonal deletion in $gp130^{F759/F759}$ mice. SEB (100 μg/mouse) was intraperitoneally injected into 6-wk-old $gp130^{F759/F759}$ (black circles) and $gp130^{WT/WT}$ (white circles) mice on day 0. Peripheral blood was collected on days 0, 3, 7, and 14. The cells were stained with FITC-anti-Vβ8.1/8.2 (a) or -anti-Vβ6 (b) and APC-anti-CD4, and analyzed by flow cytometry. The average frequencies ($n = 3$) of the specific Vβ-expressing cells in the CD4$^+$ cells are plotted. The error bars indicate SD of three mice. Asterisks indicate significant differences by Student's t test (*$P < 0.05$). Representative data from three independent experiments are shown.

Dependence of Arthritis Development on Lymphocytes. All results described above showed that there were several abnormalities of immune responses in $gp130^{F759/F759}$ mice, suggesting that abnormal immunity is critically involved in arthritis development. To clarify this issue, we investigated whether lymphocytes are actually required for the disease. To address this issue, we crossed $gp130^{F759/F759}$ mice with RAG-2–deficient mice to generate $gp130^{F759/F759}RAG\text{-}2^{-/-}$ double mutant animals as described in Materials and Methods. 81% of the $gp130^{F759/F759}RAG\text{-}2^{+/+}$ or $gp130^{F759/F759}RAG\text{-}2^{+/-}$ mutant mice (13 of 16) had developed arthritis (average score ± SEM, 9.0 ± 2.7) at 14 mo old. However, the $gp130^{F759/F759}/RAG\text{-}2^{-/-}$ mice did not develop arthritis ($n = 15$), except for one case showing only a mild, transient restriction of joints (Fig. 8). These results clearly establish that lymphocytes are essential for the development of the arthritis in the $gp130^{F759/F759}$ mice.

Discussion

Here we showed that a point mutation of Y759 in gp130 in mice caused spontaneous development of an age-dependent RA-like joint disease accompanied by autoantibody production and T cell abnormalities, including impairment of peripheral clonal deletion. Most importantly, lymphocytes were required for disease development. The arthritis in $gp130^{F759/F759}$ mice developed in middle age and its clinical course was chronic and progressive. It started

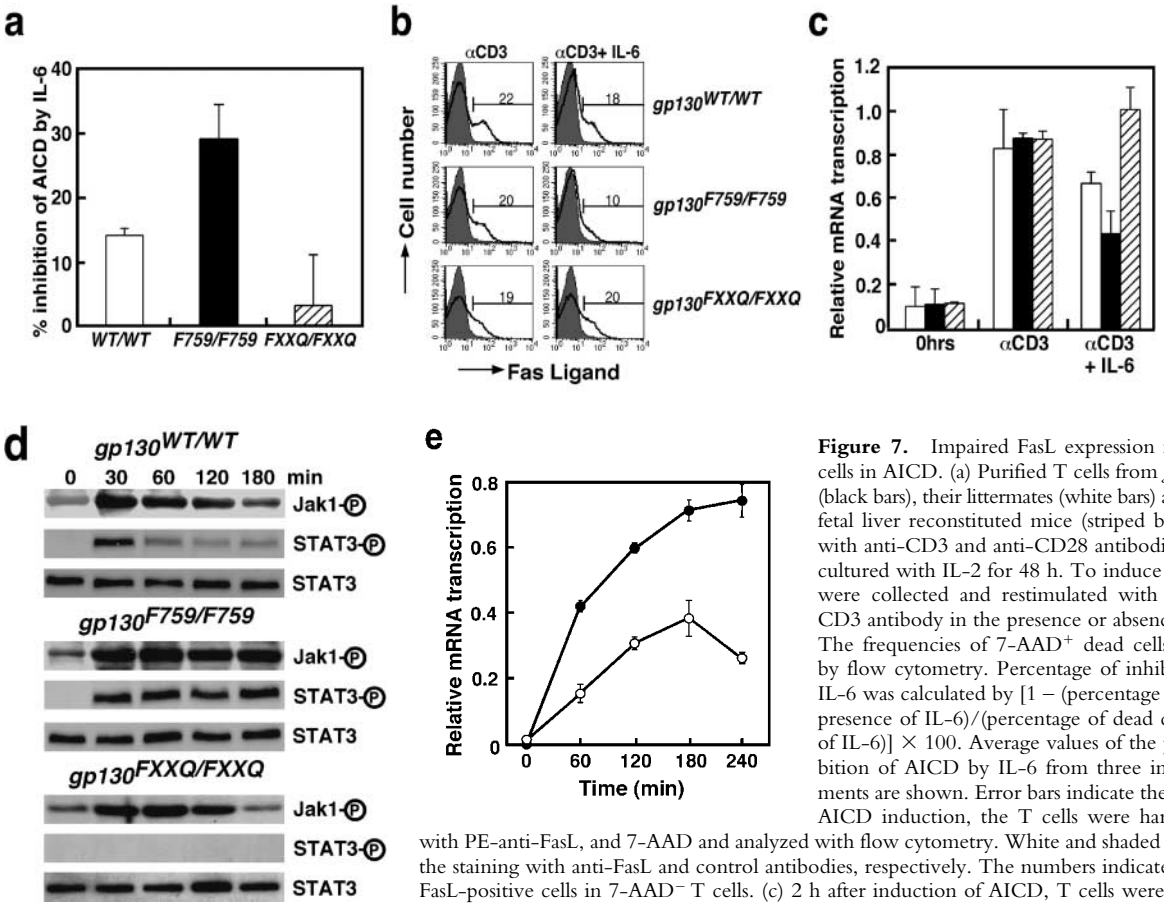

Figure 7. Impaired FasL expression in *gp130*$^{F759/F759}$ T cells in AICD. (a) Purified T cells from *gp130*$^{F759/F759}$ mice (black bars), their littermates (white bars) and *gp130*$^{FXXQ/FXXQ}$ fetal liver reconstituted mice (striped bars) were activated with anti-CD3 and anti-CD28 antibodies for 48 h and recultured with IL-2 for 48 h. To induce AICD, live T cells were collected and restimulated with immobilized anti-CD3 antibody in the presence or absence of IL-6 for 20 h. The frequencies of 7-AAD$^+$ dead cells were determined by flow cytometry. Percentage of inhibition of AICD by IL-6 was calculated by [1 − (percentage of dead cells in the presence of IL-6)/(percentage of dead cells in the absence of IL-6)] × 100. Average values of the percentage of inhibition of AICD by IL-6 from three independent experiments are shown. Error bars indicate the SEM. (b) 8 h after AICD induction, the T cells were harvested and stained with PE-anti-FasL, and 7-AAD and analyzed with flow cytometry. White and shaded histograms indicate the staining with anti-FasL and control antibodies, respectively. The numbers indicate the frequencies of FasL-positive cells in 7-AAD$^-$ T cells. (c) 2 h after induction of AICD, T cells were harvested, and the total RNA was isolated. Transcription levels of FasL mRNA were estimated by quantitative RT-PCR. The relative transcription levels of FasL mRNA in *gp130*$^{WT/WT}$ (white bars), *gp130*$^{F759/F759}$ (black bars), and *gp130*$^{FXXQ/FXXQ}$ (striped bars) T cells are indicated. The averages from three independent experiments are shown. Error bars indicate the SD. (d) Activated T cells from *gp130*$^{WT/WT}$ and *gp130*$^{F759/F759}$ mice and *gp130*$^{FXXQ/FXXQ}$ fetal liver reconstituted mice were stimulated with IL-6 for the indicated periods. Cells were lysed and immunoblotted with anti-phosphotyrosine-JAK-1, anti-phosphotyrosine-STAT-3 or anti-STAT-3 antibodies. (e) Activated T cells were stimulated with IL-6 for the indicated periods. Cells were harvested and the total RNA was isolated. Transcription levels of SOCS-3 mRNA were estimated by quantitative RT-PCR. The relative transcription levels of SOCS-3 mRNA in *gp130*$^{WT/WT}$ (white circles), and *gp130*$^{F759/F759}$ (black circles) T cells are indicated. Error bars indicate the SD.

with mild swelling and redness of the paws, and joint mobility decreased thereafter. The larger joints were affected symmetrically, and the joints eventually became ankylotic. Radiologic analysis of the affected joints revealed the characteristics of advanced human RA. Histologic examination showed leukocytes infiltrating the joint space, hyperplasia of the synovium with pannus formation, destruction of the cartilage and bone, and bony ankylosis, all of which resemble characteristics of human RA.

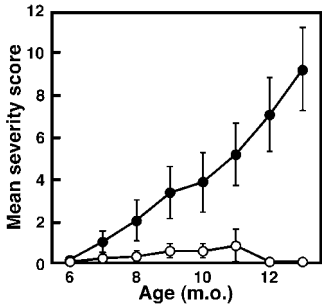

Figure 8. Lymphocytes are required for the development of arthritis. *gp130*$^{F759/F759}$*RAG-2*$^{+/-}$ or *RAG-2*$^{+/+}$ (white circles) (n = 16) and *gp130*$^{F759/F759}$*RAG-2*$^{-/-}$ (black circles) (n = 15) mice were examined and scored monthly for severity of arthritis. Data represent means ± SEM.

Foci of lymphocytes and plasma cells were scattered around periarticular regions, although the degree of infiltration of these cells was less than in human RA. The transcription of proinflammatory cytokines, in particular IL-6, in the joints was increased. Although the infiltration of lymphocytes was not marked around the joint tissues, the involvement of an immunological abnormality in the pathophysiology of the arthritis was indicated since the development of arthritis was totally dependent on lymphocytes: introduction of the *gp130*$^{F759/F759}$ mutation into RAG-2–deficient mice did not cause arthritis. This is in sharp contrast to the arthritis that develops in TNF AU-rich elements-deficient mice, which is independent of lymphocytes (9). Consistent with this notion, production of a variety of autoantibodies was observed in the diseased mice. The involvement of autoantibody in RA or experimentally induced arthritis model has been recently reconsidered (2, 7).

However, we did not observe any correlation between the level of any of autoantibody and severity, suggesting

that B cell response may be less important than T cell response. In line with the hypothesis that T cells play roles in the disease we observed several abnormlities of T cells. In the thymus of mice with arthritis, the frequency of CD4/CD8 double-positive cells decreased and that of CD4 or CD8 single-positive cells increased. In the lymph nodes of *gp130$^{F759/F759}$* mice with arthritis, a decrease in naive CD4$^+$ and CD8$^+$ T cells, and an increase in memory/activated CD4$^+$ T cells were observed. These abnormal T cell populations appeared in young mice before the onset of the disease. Functionally, the in vitro hyperresponsiveness of T cells in the thymus and lymph nodes was also observed before disease onset. The impairment of both thymic negative selection and peripheral clonal deletion suggests that self-tolerance is disrupted in *gp130$^{F759/F759}$* mice. Taken together, all results suggest that T cells may play critical roles in the development of arthritis.

Ernst et al. reported that the knock-in mouse *gp130$^{\Delta STAT/\Delta STAT}$* displays impaired acute phase and immune responses and develops severe gastrointestinal ulceration and joint disease (42). However, the joint disease that develops in Ernst's mouse is quite different from RA and the disease in our *gp130$^{F759/F759}$* mutant mouse. The most important difference is that the immune response is not involved in the development of Ernst's joint disease, in which the major mechanism seems to be a proliferative disorder of the synovial cells most likely due to enhanced ERK MAPK activation through mutated gp130. The different phenotypes generated in Ernst's mice and ours could be explained by the different mutations introduced in gp130. To make the *gp130$^{\Delta STAT/\Delta STAT}$* mouse, they deleted a large portion of the cytoplasmic domain of gp130, including the region required for STAT-3 activation. It should be noted that the deletion of such a large portion of gp130 may cause a wide range of signal transduction abnormalities, not only for STAT-3 but also for other unknown signals. On the other hand, to make the *gp130$^{F759/F759}$* mouse, we introduced point mutation at tyrosine residue Y759, which is required for negative regulation of gp130-mediated STAT-3 activation by the SHP2-mediated signal transduction and/or SOCS-3–mediated negative feedback (31–33); thus, our mutant *gp130$^{F759/F759}$* mouse is completely distinct from Ernst's gp130 mutant mouse.

Analysis using the H-Y system revealed that thymic negative selection was almost normal in the *gp130$^{F759/F759}$* mice, except for an increase in CD8^{lo} cells. It has been reported that substantially self-reactive clones with TCRs that have low avidity to self-antigen escape negative selection (43). These clones are not completely anergic to self-antigens and can respond to the antigen if it is abundant. Thus, an intriguing hypothesis is that autoreactive T cell clones with low-avidity TCRs for self-antigens escape the thymic selection of *gp130$^{F759/F759}$* mice, and that they are activated when the self-antigens become available due to certain age-dependent changes in the microenvironment. In addition to thymic selection, the clonal deletion of activated T cells in the periphery is important to maintain self-tolerance (37, 44). After SEB injection, the number of responsive CD4$^+$ Vβ8$^+$ T cells in the peripheral blood was reduced in wild-type but not *gp130$^{F759/F759}$* mice, demonstrating the impairment of clonal deletion in the *gp130$^{F759/F759}$* mice in vivo. Several reports indicated that IL-6 has antiapoptotic effects on naive but not activated T cells (45–47), and the inhibition of AICD and downregulation of FasL by IL-6 has been reported previously (48). IL-6 only slightly inhibited AICD and anti-CD3–induced upregulation of FasL in activated wild-type T cells. Importantly, this negative effect on FasL expression was enhanced in *gp130$^{F759/F759}$* compared with wild-type T cells, whereas IL-6 had no effect on *gp130$^{FXXQ/FXXQ}$* T cells. Because IL-6–induced activation of STAT-3 was prolonged in *gp130$^{F759/F759}$* T cells, while IL-6 failed to activate STAT-3 in *gp130$^{FXXQ/FXXQ}$* T cells, it is most likely that STAT-3 has a suppressive effect on the anti-CD3–induced upregulation of FasL in activated T cells.

It is also possible that unknown signals generated from any one of the four tyrosine residues of gp130 that are required for STAT-3 activation may be involved in the suppression of FasL expression. Alternatively SOCS-3 may interfere T cell receptor-mediated signaling involved in FasL induction since IL-6–mediated SOCS-3 induction was enhanced in *gp130$^{F759/F759}$* T cells as compared with wild-type T cells. In any case, it is evident that *gp130$^{F759/F759}$* T cells showed suppressed FasL expression in the presence of IL-6 in a manner dependent on the tyrosine residues of gp130 that are required for STAT-3 activation. Regardless of the precise mechanism, it is reasonable to speculate that resistance of T cells in *gp130$^{F759/F759}$* mice to clonal deletion in vivo is also involved in the development of autoimmune disease by the breakdown of self-tolerance. An intriguing possibility is that very mild impairment of both central and peripheral tolerance is required for the development of age-dependent autoimmune disease in *gp130$^{F759/F759}$* mice. Study of the signal transduction pathways that are initiated through gp130 has shown that a single cytokine receptor can simultaneously transduce multiple, contradictory signals, leading to a variety of responses, such as growth and differentiation, and that the balance of the contradictory signals determines the biological output of a given cytokine (24).

The fact that selective disruption of gp130 signals dependent on Y759, which augments gp130-mediated STAT-3 activation (33), resulted in joint disease with autoimmunity, provides an intriguing, unique case where the disruption of the balance of signals transduced from one cytokine receptor may cause autoimmune disease. It is also possible that lack of negative feedback mechanisms through SOCS-3 may be involved in enhanced STAT-3 activation through gp130 and the generation of the disease, since Y759 is shown to be required for the negative effect of SOCS-3 (31, 32). Another possibility is that enhanced induction of SOCS-3 through gp130 may modulate signaling by other cytokines.

Although we clearly showed that lymphocytes are required for disease development, it is also possible that abnormal gp130-mediated signals generated in other cells

function with lymphocytes to cause diseases because gp130 is expressed in a variety of cells, including macrophages, granulocytes, dendritic cells, fibroblasts, epithelial cells, endothelial cells, synovial cells, and osteoclasts. Among them, granulocytes infiltrating in the synovium may play an important role in the course of arthritis.

Taken together, our results show that the *gp130*$^{F759/F759}$ mutant mouse is a new animal model of autoimmune arthritis and is unique in demonstrating that a point mutation of a cytokine receptor can trigger complicated immunological and inflammatory processes, leading to the generation of autoimmune disease.

We thank Ms. R. Masuda and A. Kubota for secretarial assistance. We also thank Drs. Y. Iwakura, S. Saijo, and M. Sasai for their kind advice regarding the analyses of the arthritis, Dr. Y. Takahama for the FITC-T3.70 mAb, and Dr. M. Itoh for the B6.RAG-2–deficient mice. We thank Dr. M. Murakami for critical reading and suggestions.

This work is supported by a grant-in-aid for scientific research from the Ministry of Education, Culture, Sports, Science, and Technology in Japan, and the Osaka Foundation for the Promotion of Clinical Immunology.

Submitted: 17 April 2002
Revised: 12 August 2002
Accepted: 21 August 2002

References

1. Feldmann, M., F.M. Brennan, and R.N. Maini. 1996. Rheumatoid arthritis. *Cell.* 85:307–310.
2. Hirano, T. 2002. Revival of the autoantibody model in rheumatoid arthritis. *Nat. Immunol.* 3:342–344.
3. Feldmann, M., F.M. Brennan, and R.N. Maini. 1996. Role of cytokines in rheumatoid arthritis. *Annu. Rev. Immunol.* 14: 397–440.
4. Hirano, T. 1998. Interleukin 6 and its receptor: ten years later. *Int. Rev. Immunol.* 16:249–284.
5. O'Shea, J.J., A. Ma, and P. Lipsky. 2002. Cytokines and autoimmunity. *Nat. Rev. Immunol.* 2:37–45.
6. Kouskoff, V., A.S. Korganow, V. Duchatelle, C. Degott, C. Benoist, and D. Mathis. 1996. Organ-specific disease provoked by systemic autoimmunity. *Cell.* 87:811–822.
7. Matsumoto, I., A. Staub, C. Benoist, and D. Mathis. 1999. Arthritis provoked by linked T and B cell recognition of a glycolytic enzyme. *Science.* 286:1732–1735.
8. Iwakura, Y., M. Tosu, E. Yoshida, M. Takiguchi, K. Sato, I. Kitajima, K. Nishioka, K. Yamamoto, T. Takeda, M. Hatanaka, et al. 1991. Induction of inflammatory arthropathy resembling rheumatoid arthritis in mice transgenic for HTLV-I. *Science.* 253:1026–1028.
9. Kontoyiannis, D., M. Pasparakis, T.T. Pizarro, F. Cominelli, and G. Kollias. 1999. Impaired on/off regulation of TNF biosynthesis in mice lacking TNF AU-rich elements: implications for joint and gut-associated immunopathologies. *Immunity.* 10:387–398.
10. Keffer, J., L. Probert, H. Cazlaris, S. Georgopoulos, E. Kaslaris, D. Kioussis, and G. Kollias. 1991. Transgenic mice expressing human tumour necrosis factor: a predictive genetic model of arthritis. *EMBO J.* 10:4025–4031.
11. Niki, Y., H. Yamada, S. Seki, T. Kikuchi, H. Takaishi, Y. Toyama, K. Fujikawa, and N. Tada. 2001. Macrophage- and neutrophil-dominant arthritis in human IL-1α transgenic mice. *J. Clin. Invest.* 107:1127–1135.
12. Horai, R., S. Saijo, H. Tanioka, S. Nakae, K. Sudo, A. Okahara, T. Ikuse, M. Asano, and Y. Iwakura. 2000. Development of chronic inflammatory arthropathy resembling rheumatoid arthritis in interleukin 1 receptor antagonist-deficient mice. *J. Exp. Med.* 191:313–320.
13. Teranishi, T., T. Hirano, N. Arima, and K. Onoue. 1982. Human helper T cell factor(s) (ThF). II. Induction of IgG production in B lymphoblastoid cell lines and identification of T cell-replacing factor-(TRF) like factor(s). *J. Immunol.* 128:1903–1908.
14. Hirano, T., K. Yasukawa, H. Harada, T. Taga, Y. Watanabe, T. Matsuda, S. Kashiwamura, K. Nakajima, K. Koyama, A. Iwamatsu, et al. 1986. Complementary DNA for a novel human interleukin (BSF-2) that induces B lymphocytes to produce immunoglobulin. *Nature.* 324:73–76.
15. Van Snick, J. 1990. Interleukin-6: an overview. *Annu. Rev. Immunol.* 8:253–278.
16. Hirano, T., T. Taga, K. Yasukawa, K. Nakajima, N. Nakano, F. Takatsuki, M. Shimizu, A. Murashima, S. Tsunasawa, F. Sakiyama, et al. 1987. Human B-cell differentiation factor defined by an anti-peptide antibody and its possible role in autoantibody production. *Proc. Natl. Acad. Sci. USA.* 84:228–231.
17. Hirano, T., T. Matsuda, M. Turner, N. Miyasaka, G. Buchan, B. Tang, K. Sato, M. Shimizu, R. Maini, M. Feldmann, et al. 1988. Excessive production of interleukin 6/B cell stimulatory factor-2 in rheumatoid arthritis. *Eur. J. Immunol.* 18:1797–1801.
18. Alonzi, T., E. Fattori, D. Lazzaro, P. Costa, L. Probert, G. Kollias, F. De Benedetti, V. Poli, and G. Ciliberto. 1998. Interleukin 6 is required for the development of collagen-induced arthritis. *J. Exp. Med.* 187:461–468.
19. Sasai, M., Y. Saeki, S. Ohshima, K. Nishioka, T. Mima, T. Tanaka, Y. Katada, K. Yoshizaki, M. Suemura, and T. Kishimoto. 1999. Delayed onset and reduced severity of collagen-induced arthritis in interleukin-6-deficient mice. *Arthr. Rheum.* 42:1635–1643.
20. Ohshima, S., Y. Saeki, T. Mima, M. Sasai, K. Nishioka, S. Nomura, M. Kopf, Y. Katada, T. Tanaka, M. Suemura, and T. Kishimoto. 1998. Interleukin 6 plays a key role in the development of antigen-induced arthritis. *Proc. Natl. Acad. Sci. USA.* 95:8222–8226.
21. Samoilova, E.B., J.L. Horton, B. Hilliard, T.S. Liu, and Y. Chen. 1998. IL-6-deficient mice are resistant to experimental autoimmune encephalomyelitis: roles of IL-6 in the activation and differentiation of autoreactive T cells. *J. Immunol.* 161:6480–6486.
22. Eugster, H.P., K. Frei, M. Kopf, H. Lassmann, and A. Fontana. 1998. IL-6-deficient mice resist myelin oligodendrocyte glycoprotein-induced autoimmune encephalomyelitis. *Eur. J. Immunol.* 28:2178–2187.
23. Richards, H.B., M. Satoh, M. Shaw, C. Libert, V. Poli, and W.H. Reeves. 1998. Interleukin 6 dependence of anti-DNA antibody production: evidence for two pathways of autoantibody formation in pristane-induced lupus. *J. Exp. Med.* 188: 985–990.
24. Hirano, T., K. Nakajima, and M. Hibi. 1997. Signaling mechanisms through gp130: a model of the cytokine system. *Cytokine Growth Factor Rev.* 8:241–252.
25. Hirano, T., K. Ishihara, and M. Hibi. 2000. Roles of STAT3

in mediating the cell growth, differentiation and survival signals relayed through the IL-6 family of cytokine receptors. *Oncogene*. 19:2548–2556.
26. Hibi, M., and T. Hirano. 2000. Gab-family adapter molecules in signal transduction of cytokine and growth factor receptors, and T and B cell antigen receptors. *Leuk. Lymphoma*. 37:299–307.
27. Fukada, T., M. Hibi, Y. Yamanaka, M. Takahashi-Tezuka, Y. Fujitani, T. Yamaguchi, K. Nakajima, and T. Hirano. 1996. Two signals are necessary for cell proliferation induced by a cytokine receptor gp130: involvement of STAT3 in anti-apoptosis. *Immunity*. 5:449–460.
28. Nakajima, K., Y. Yamanaka, K. Nakae, H. Kojima, M. Ichiba, N. Kiuchi, T. Kitaoka, T. Fukada, M. Hibi, and T. Hirano. 1996. A central role for Stat3 in IL-6-induced regulation of growth and differentiation in M1 leukemia cells. *EMBO J.* 15:3651–3658.
29. Sengupta, T.K., E.S. Talbot, P.A. Scherle, and L.B. Ivashkiv. 1998. Rapid inhibition of interleukin-6 signaling and Stat3 activation mediated by mitogen-activated protein kinases. *Proc. Natl. Acad. Sci. USA*. 95:11107–11112.
30. Jain, N., T. Zhang, S.L. Fong, C.P. Lim, and X. Cao. 1998. Repression of Stat3 activity by activation of mitogen-activated protein kinase (MAPK). *Oncogene*. 17:3157–3167.
31. Nicholson, S.E., D. De Souza, L.J. Fabri, J. Corbin, T.A. Willson, J.G. Zhang, A. Silva, M. Asimakis, A. Farley, A.D. Nash, et al. 2000. Suppressor of cytokine signaling-3 preferentially binds to the SHP-2-binding site on the shared cytokine receptor subunit gp130. *Proc. Natl. Acad. Sci. USA*. 97: 6493–6498.
32. Schmitz, J., M. Weissenbach, S. Haan, P.C. Heinrich, and F. Schaper. 2000. SOCS3 exerts its inhibitory function on interleukin-6 signal transduction through the SHP2 recruitment site of gp130. *J. Biol. Chem.* 275:12848–12856.
33. Ohtani, T., K. Ishihara, T. Atsumi, K. Nishida, Y. Kaneko, T. Miyata, S. Itoh, M. Narimatsu, H. Maeda, T. Fukada, et al. 2000. Dissection of signaling cascades through gp130 in vivo: reciprocal roles for STAT3- and SHP2-mediated signals in immune responses. *Immunity*. 12:95–105.
34. Itoh, M., K. Ishihara, T. Hiroi, B.O. Lee, H. Maeda, H. Iijima, M. Yanagita, H. Kiyono, and T. Hirano. 1998. Deletion of bone marrow stromal cell antigen-1 (CD157) gene impaired systemic thymus independent-2 antigen-induced IgG3 and mucosal TD antigen-elicited IgA responses. *J. Immunol.* 161:3974–3983.
35. Overbergh, L., D. Valckx, M. Waer, and C. Mathieu. 1999. Quantification of murine cytokine mRNAs using real time quantitative reverse transcriptase PCR. *Cytokine*. 11:305–312.
36. Ishihara, K., Y. Kobune, Y. Okuyama, M. Itoh, B.O. Lee, O. Muraoka, and T. Hirano. 1996. Stage-specific expression of mouse BST-1/BP-3 on the early B and T cell progenitors prior to gene rearrangement of antigen receptor. *Int. Immunol.* 8:1395–1404.
37. Van Parijs, L., and A.K. Abbas. 1998. Homeostasis and self-tolerance in the immune system: turning lymphocytes off. *Science*. 280:243–248.
38. Kamradt, T., and N.A. Mitchison. 2001. Tolerance and autoimmunity. *N. Engl. J. Med*. 344:655–664.
39. Kisielow, P., H. Bluthmann, U.D. Staerz, M. Steinmetz, and H. von Boehmer. 1988. Tolerance in T-cell-receptor transgenic mice involves deletion of nonmature $CD4^+8^+$ thymocytes. *Nature*. 333:742–746.
40. Teh, H.S., H. Kishi, B. Scott, and H. Von Boehmer. 1989. Deletion of autospecific T cells in T cell receptor (TCR) transgenic mice spares cells with normal TCR levels and low levels of CD8 molecules. *J. Exp. Med*. 169:795–806.
41. Kawabe, Y., and A. Ochi. 1991. Programmed cell death and extrathymic reduction of $V\beta8^+$ $CD4^+$ T cells in mice tolerant to Staphylococcus aureus enterotoxin B. *Nature*. 349: 245–248.
42. Ernst, M., M. Inglese, P. Waring, I.K. Campbell, S. Bao, F.J. Clay, W.S. Alexander, I.P. Wicks, D.M. Tarlinton, U. Novak, et al. 2001. Defective gp130-mediated signal transducer and activator of transcription (STAT) signaling results in degenerative joint disease, gastrointestinal ulceration, and failure of uterine implantation. *J. Exp. Med*. 194:189–204.
43. Bouneaud, C., P. Kourilsky, and P. Bousso. 2000. Impact of negative selection on the T cell repertoire reactive to a self-peptide: a large fraction of T cell clones escapes clonal deletion. *Immunity*. 13:829–840.
44. Janssen, O., R. Sanzenbacher, and D. Kabelitz. 2000. Regulation of activation-induced cell death of mature T-lymphocyte populations. *Cell Tiss. Res*. 301:85–99.
45. Teague, T.K., P. Marrack, J.W. Kappler, and A.T. Vella. 1997. IL-6 rescues resting mouse T cells from apoptosis. *J. Immunol*. 158:5791–5796.
46. Takeda, K., T. Kaisho, N. Yoshida, J. Takeda, T. Kishimoto, and S. Akira. 1998. Stat3 activation is responsible for IL-6-dependent T cell proliferation through preventing apoptosis: generation and characterization of T cell- specific Stat3-deficient mice. *J. Immunol*. 161:4652–4660.
47. Narimatsu, M., H. Maeda, S. Itoh, T. Atsumi, T. Ohtani, K. Nishida, M. Itoh, D. Kamimura, S.J. Park, K. Mizuno, et al. 2001. Tissue-specific autoregulation of the Stat3 gene and its role in interleukin-6-induced survival signals in T cells. *Mol. Cell. Biol*. 21:6615–6625.
48. Ayroldi, E., O. Zollo, L. Cannarile, F. D'Adamio, U. Grohmann, D.V. Delfino, and C. Riccardi. 1998. Interleukin-6 (IL-6) prevents activation-induced cell death: IL-2-independent inhibition of Fas/FasL expression and cell death. *Blood*. 92:4212–4219.